Disappearance of back-to-back high p_T hadron correlations in central Au+Au collisions at $\sqrt{s_{NN}} = 200$ GeV

C. Adler[11], Z. Ahammed[23], C. Allgower[12], J. Amonett[14], B.D. Anderson[14], M. Anderson[5], G.S. Averichev[9], J. Balewski[12], O. Barannikova[9,23], L.S. Barnby[14], J. Baudot[13], S. Bekele[20], V.V. Belaga[9], R. Bellwied[31], J. Berger[11], H. Bichsel[30], A. Billmeier[31], L.C. Bland[2], C.O. Blyth[3], B.E. Bonner[24], A. Boucham[26], A. Brandin[18], A. Bravar[2], R.V. Cadman[1], H. Caines[33], M. Calderón de la Barca Sánchez[2], A. Cardenas[23], J. Carroll[15], J. Castillo[26], M. Castro[31], D. Cebra[5], P. Chaloupka[20], S. Chattopadhyay[31], Y. Chen[6], S.P. Chernenko[9], M. Cherney[8], A. Chikanian[33], B. Choi[28], W. Christie[2], J.P. Coffin[13], T.M. Cormier[31], M.M. Corral[16], J.G. Cramer[30], H.J. Crawford[4], A.A. Derevschikov[22], L. Didenko[2], T. Dietel[11], J.E. Draper[5], V.B. Dunin[9], J.C. Dunlop[33], V. Eckardt[16], L.G. Efimov[9], V. Emelianov[18], J. Engelage[4], G. Eppley[24], B. Erazmus[26], P. Fachini[2], V. Faine[2], J. Faivre[13], R. Fatemi[12], K. Filimonov[15], E. Finch[33], Y. Fisyak[2], D. Flierl[11], K.J. Foley[2], J. Fu[15,32], C.A. Gagliardi[27], N. Gagunashvili[9], J. Gans[33], L. Gaudichet[26], M. Germain[13], F. Geurts[24], V. Ghazikhanian[6], O. Grachov[31], V. Grigoriev[18], M. Guedon[13], E. Gushin[18], T.J. Hallman[2], D. Hardtke[15], J.W. Harris[33], T.W. Henry[27], S. Heppelmann[21], T. Herston[23], B. Hippolyte[13], A. Hirsch[23], E. Hjort[15], G.W. Hoffmann[28], M. Horsley[33], H.Z. Huang[6], T.J. Humanic[20], G. Igo[6], A. Ishihara[28], Yu.I. Ivanshin[10], P. Jacobs[15], W.W. Jacobs[12], M. Janik[29], I. Johnson[15], P.G. Jones[3], E.G. Judd[4], M. Kaneta[15], M. Kaplan[7], D. Keane[14], J. Kiryluk[6], A. Kisiel[29], J. Klay[15], S.R. Klein[15], A. Klyachko[12], T. Kollegger[11], A.S. Konstantinov[22], M. Kopytine[14], L. Kotchenda[18], A.D. Kovalenko[9], M. Kramer[19], P. Kravtsov[18], K. Krueger[1], C. Kuhn[13], A.I. Kulikov[9], G.J. Kunde[33], C.L. Kunz[7], R.Kh. Kutuev[10], A.A. Kuznetsov[9], L. Lakehal-Ayat[26], M.A.C. Lamont[3], J.M. Landgraf[2], S. Lange[11], C.P. Lansdell[28], B. Lasiuk[33], F. Laue[2], J. Lauret[2], A. Lebedev[2], R. Lednický[9], V.M. Leontiev[22], M.J. LeVine[2], Q. Li[31], S.J. Lindenbaum[19], M.A. Lisa[20], F. Liu[32], L. Liu[32], Z. Liu[32], Q.J. Liu[30], T. Ljubicic[2], W.J. Llope[24], G. LoCurto[16], H. Long[6], R.S. Longacre[2], M. Lopez-Noriega[20], W.A. Love[2], T. Ludlam[2], D. Lynn[2], J. Ma[6], D. Magestro[20], R. Majka[33], S. Margetis[14], C. Markert[33], L. Martin[26], J. Marx[15], H.S. Matis[15], Yu.A. Matulenko[22], T.S. McShane[8], F. Meissner[15], Yu. Melnick[22], A. Meschanin[22], M. Messer[2], M.L. Miller[33], Z. Milosevich[7], N.G. Minaev[22], J. Mitchell[24], C.F. Moore[28], V. Morozov[15], M.M. de Moura[31], M.G. Munhoz[25], J.M. Nelson[3], P. Nevski[2], V.A. Nikitin[10], L.V. Nogach[22], B. Norman[14], S.B. Nurushev[22], G. Odyniec[15], A. Ogawa[21], V. Okorokov[18], M. Oldenburg[16], D. Olson[15], G. Paic[20], S.U. Pandey[31], Y. Panebratsev[9], S.Y. Panitkin[2], A.I. Pavlinov[31], T. Pawlak[29], V. Perevoztchikov[2], W. Peryt[29], V.A Petrov[10], M. Planinic[12], J. Pluta[29], N. Porile[23], J. Porter[2], A.M. Poskanzer[15], E. Potrebenikova[9], D. Prindle[30], C. Pruneau[31], J. Putschke[16], G. Rai[15], G. Rakness[12], O. Ravel[26], R.L. Ray[28], S.V. Razin[9,12], D. Reichhold[8], J.G. Reid[30], G. Renault[26], F. Retiere[15], A. Ridiger[18], H.G. Ritter[15], J.B. Roberts[24], O.V. Rogachevski[9], J.L. Romero[5], A. Rose[31], C. Roy[26], V. Rykov[31], I. Sakrejda[15], S. Salur[33], J. Sandweiss[33], I. Savin[10], J. Schambach[28], R.P. Scharenberg[23], N. Schmitz[16], L.S. Schroeder[15], A. Schüttauf[16], K. Schweda[15], J. Seger[8], D. Seliverstov[18], P. Seyboth[16], E. Shahaliev[9], K.E. Shestermanov[22], S.S. Shimanskii[9], F. Simon[16], G. Skoro[9], N. Smirnov[33], R. Snellings[15], P. Sorensen[6], J. Sowinski[12], H.M. Spinka[1], B. Srivastava[23], E.J. Stephenson[12], R. Stock[11], A. Stolpovsky[31], M. Strikhanov[18], B. Stringfellow[23], C. Struck[11], A.A.P. Suaide[31], E. Sugarbaker[20], C. Suire[2], M. Šumbera[20], B. Surrow[2], T.J.M. Symons[15], A. Szanto de Toledo[25], P. Szarwas[29], A. Tai[6], J. Takahashi[25], A.H. Tang[15], D. Thein[6], J.H. Thomas[15], M. Thompson[3], V. Tikhomirov[18], M. Tokarev[9], M.B. Tonjes[17], T.A. Trainor[30], S. Trentalange[6], R.E. Tribble[27], V. Trofimov[18], O. Tsai[6], T. Ullrich[2], D.G. Underwood[1], G. Van Buren[2], A.M. VanderMolen[17], I.M. Vasilevski[10], A.N. Vasiliev[22], S.E. Vigdor[12], S.A. Voloshin[31], F. Wang[23], H. Ward[28], J.W. Watson[14], R. Wells[20], G.D. Westfall[17], C. Whitten Jr. [6], H. Wieman[15], R. Willson[20], S.W. Wissink[12], R. Witt[33], J. Wood[6], N. Xu[15], Z. Xu[2], A.E. Yakutin[22], E. Yamamoto[15], J. Yang[6], P. Yepes[24], V.I. Yurevich[9], Y.V. Zanevski[9], I. Zborovský[9], H. Zhang[33], W.M. Zhang[14], R. Zoulkarneev[10], A.N. Zubarev[9]

(STAR Collaboration)

[1]Argonne National Laboratory, Argonne, Illinois 60439

[2]Brookhaven National Laboratory, Upton, New York 11973

[3]University of Birmingham, Birmingham, United Kingdom

[4]University of California, Berkeley, California 94720

[5]University of California, Davis, California 95616

[6]University of California, Los Angeles, California 90095

[7]Carnegie Mellon University, Pittsburgh, Pennsylvania 15213

[8]Creighton University, Omaha, Nebraska 68178

[9]Laboratory for High Energy (JINR), Dubna, Russia
[10]Particle Physics Laboratory (JINR), Dubna, Russia
[11]University of Frankfurt, Frankfurt, Germany
[12]Indiana University, Bloomington, Indiana 47408
[13]Institut de Recherches Subatomiques, Strasbourg, France
[14]Kent State University, Kent, Ohio 44242
[15]Lawrence Berkeley National Laboratory, Berkeley, California 94720
[16]Max-Planck-Institut fuer Physik, Munich, Germany
[17]Michigan State University, East Lansing, Michigan 48824
[18]Moscow Engineering Physics Institute, Moscow Russia
[19]City College of New York, New York City, New York 10031
[20]Ohio State University, Columbus, Ohio 43210
[21]Pennsylvania State University, University Park, Pennsylvania 16802
[22]Institute of High Energy Physics, Protvino, Russia
[23]Purdue University, West Lafayette, Indiana 47907
[24]Rice University, Houston, Texas 77251
[25]Universidade de Sao Paulo, Sao Paulo, Brazil
[26]SUBATECH, Nantes, France
[27]Texas A&M University, College Station, Texas 77843
[28]University of Texas, Austin, Texas 78712
[29]Warsaw University of Technology, Warsaw, Poland
[30]University of Washington, Seattle, Washington 98195
[31]Wayne State University, Detroit, Michigan 48201
[32]Institute of Particle Physics, CCNU (HZNU), Wuhan, 430079 China
[33]Yale University, New Haven, Connecticut 06520

Azimuthal correlations for large transverse momentum charged hadrons have been measured over a wide pseudo-rapidity range and full azimuth in Au+Au and p+p collisions at $\sqrt{s_{NN}} = 200$ GeV. The small-angle correlations observed in p+p collisions and at all centralities of Au+Au collisions are characteristic of hard-scattering processes already observed in elementary collisions. A strong back-to-back correlation exists for p+p and peripheral Au + Au. In contrast, the back-to-back correlations are reduced considerably in the most central Au+Au collisions, indicating substantial interaction as the hard-scattered partons or their fragmentation products traverse the medium.

PACS numbers: 25.75

In collisions of heavy nuclei at high energies, a new state of matter consisting of deconfined quarks and gluons at high density is expected [1]. Large transverse momentum partons in the high-density system result from the initial hard scattering of nucleon constituents. After a hard scattering, the parton fragments to create a high energy cluster (jet) of particles. A high momentum parton traversing a dense colored medium is predicted to experience substantial energy loss [2, 3] and may be absorbed. Measurement of the parton fragmentation products after hard-scattering processes in nuclear collisions may reveal effects due to the interaction of high-momentum partons traversing the medium, thereby measuring the gluon density of the medium [4].

Hard scattering processes have been established at high transverse momentum (p_T) in elementary collisions at high energy through the measurement of jets [5, 6, 7], correlated back-to-back jets (di-jets) [8], high p_T single particles, and back-to-back correlations between high p_T hadrons [9]. Jets have been shown to carry the momentum of the parent parton [10]. The jet cross sections and high p_T single particle spectra are well described over a broad range of energies [11] in terms of the hadron's parton distributions, hard parton scattering treated by perturbative QCD, and subsequent fragmentation of the parton. High p_T jet events have also been studied in proton-nucleus interactions [12]. In the absence of effects of the nuclear medium the rate of hard processes should scale linearly with the number of binary nucleon-nucleon collisions. Recent results from RHIC, however, show a suppression of the single particle inclusive spectra of hadrons for $p_T > 2$ GeV/c in central Au+Au collisions, indicating substantial in-medium interactions [13, 14].

In this Letter, we report measurements of two-hadron angular correlations at large transverse momentum for p+p and Au+Au collisions at $\sqrt{s_{NN}} = 200$ GeV. These correlation measurements provide the most direct evidence for production of jets in high energy nucleus-nucleus collisions, and allow for the first time measurements, inaccessible in inclusive spectra, of the fate of back-to-back jets in the dense medium as a function of the size of the overlapping system. The results reveal

significant interaction of hard-scattered partons (or their fragmentation products) in the medium, with a strong dependence on the geometry and distance of traversal.

The measurements were made using the STAR detector [15] at the Relativistic Heavy-Ion Collider (RHIC) at Brookhaven National Laboratory. The STAR detector is a large acceptance magnetic spectrometer, with a large volume Time Projection Chamber (TPC) inside a 0.5 Tesla solenoidal magnet. The TPC measures the trajectories of charged particles and determines the particle momenta. The TPC has full azimuthal coverage over a pseudo-rapidity range $|\eta| < 1.5$. STAR has excellent position and momentum resolution, and, due to its vertexing capabilities, is able to identify many sources of secondary particles. The p+p analysis uses ≈10 million minimum bias p+p events triggered on the coincidence of signals from scintillator annuli spanning the pseudo-rapidity interval $3.5 \leq |\eta| \leq 5.0$. The Au+Au analysis uses ≈1.7 million minimum bias Au+Au events and ≈1.5 million top 10% central Au+Au events.

Partons fragment into jets of hadrons in a cone around the direction of the original hard-scattered parton. The leading hadron in the jet tends to be most closely aligned with the original parton direction [16]. The large multiplicities in Au+Au collisions make full jet reconstruction impractical. Thus, we utilize two-particle azimuthal correlations of high p_T charged hadrons [17] to identify jets on a statistical basis, with known sources of background correlations subtracted.

Events with at least one large transverse momentum hadron ($4 < p_T^{trig} < 6$ or $3 < p_T^{trig} < 4$ GeV/c), defined to be a *trigger* particle, are used in this analysis. For each of the trigger particles in the event, we increment the number $N(\Delta\phi, \Delta\eta)$ of *associated* tracks with 2 GeV/c $< p_T < p_T^{trig}$ as a function of their azimuthal ($\Delta\phi$) and pseudo-rapidity ($\Delta\eta$) separations from the trigger particle. We then construct an overall azimuthal pair distribution per trigger particle,

$$D(\Delta\phi) \equiv \frac{1}{N_{trigger}} \frac{1}{\epsilon} \int d\Delta\eta N(\Delta\phi, \Delta\eta), \qquad (1)$$

where $N_{trigger}$ is the observed number of tracks satisfying the trigger requirement. The efficiency ϵ for finding the associated particle is evaluated by embedding simulated tracks in real data. In order to have a high and constant tracking efficiency, the tracks are required to have $|\eta| < 0.7$, which translates to a relative pseudo-rapidity acceptance of $|\Delta\eta| < 1.4$. The single track reconstruction efficiency varies from 77% for the most central Au+Au collisions to 90% for the most peripheral Au+Au collisions and p+p collisions.

Identical analysis procedures are applied to the p+p and Au+Au data. Displayed in Figure 1 are the azimuthal distributions for same-sign and opposite-sign charged pairs from the a) p+p data and b) minimum bias Au+Au data for $4 < p_T^{trig} < 6$ GeV/c. The data are integrated over the relative pseudo-rapidity range $0 < |\Delta\eta| < 1.4$. Clear correlation peaks are observed

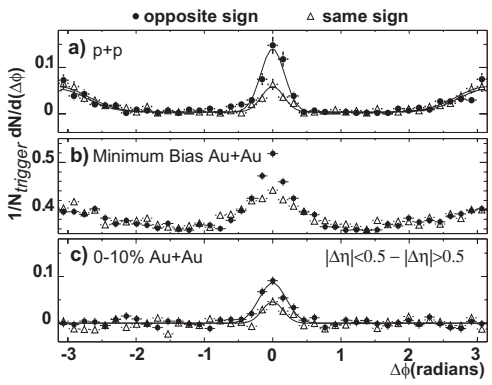

FIG. 1: Azimuthal distributions of same-sign and opposite-sign pairs for a) p+p, b) minimum bias Au+Au, and c) background-subtracted central Au+Au collisions. All correlation functions require a trigger particle with $4 < p_T^{trig} < 6$ GeV/c and associated particles with 2 GeV/c $< p_T < p_T^{trig}$. The curves are one- or two- Gaussian fits.

near $\Delta\phi \sim 0$ and $\Delta\phi \sim \pi$ in the data. The opposite-sign correlations at small relative azimuth are larger than those of the same-sign particle pairs, while the sign has a negligible effect on the back-to-back correlations.

To isolate the jet-like correlations (localized in $\Delta\phi$, $\Delta\eta$) in central Au+Au collisions, the azimuthal distributions are measured for two regions of relative pseudo-rapidity, $|\Delta\eta| < 0.5$ and $0.5 < |\Delta\eta| < 1.4$ [17]. The difference between the small and large relative pseudo-rapidity azimuthal distributions is displayed in Figure 1c along with single Gaussian fits. Near $\Delta\phi = 0$, the azimuthal distributions from Au+Au and p+p have similar shapes. For the opposite-sign azimuthal distributions, the Gaussian widths are $0.17 \pm 0.01(stat.) \pm 0.03(sys.)$ radians for p+p data, and $0.20 \pm 0.02(stat.) \pm 0.03(sys.)$ radians for the central Au+Au data. For the same-sign azimuthal distributions, the Gaussian widths are $0.16 \pm 0.02(stat.) \pm 0.03(sys.)$ radians for p+p data, and $0.15 \pm 0.03(stat.) \pm 0.04(sys.)$ radians for the central Au+Au data. The systematic errors reflect the spread of values found for different choices of the $\Delta\phi$ bin width. Within the errors, there are no significant differences between the small-angle correlation widths for p+p and central Au+Au collisions.

The ratios of the opposite-sign to same-sign peak areas are $2.7 \pm 0.9(stat.) \pm 0.2(sys.)$ for p+p and $2.5 \pm 0.6(stat.) \pm 0.2(sys.)$ for central Au+Au collisions. In jet fragmentation, there are dynamical charge correlations between the leading and next-to-leading charged hadrons [18] that originate from the formation of $q\bar{q}$ pairs along a string between two partons. This results in a preferential ordering into oppositely-charged adjacent particles along a string during fragmentation. The Hijing event generator, which utilizes the Lund string fragmentation scheme [19] incorporating these concepts, predicts a ratio of 2.6 ± 0.7 for the opposite-sign to same-sign correlation

strengths. The agreement of this ratio with those measured in the central Au+Au and p+p suggests that the same jet production mechanism is responsible for a majority of the charged hadrons with $p_T > 4$ GeV/c in p+p and central Au+Au collisions.

The decay of resonances would also lead to small-angle azimuthal correlations, but a resonance decay origin is unlikely due to the observed correlation of particles with the same charge sign, the similarity in the measured small-angle azimuthal correlation widths in the Au+Au and p+p interactions, and the strong back-to-back correlations of large p_T particles seen for p+p collisions in Fig. 1a. The latter correlations, indicative of di-jet events [9], are removed from the central Au+Au sample by the subtraction in Fig. 1c. A quantitative analysis of back-to-back jet survival in Au+Au requires the more detailed treatment of background correlations described below.

In addition to correlations due to jets, the two-particle azimuthal distributions in Au+Au exhibit a structure attributable to an anisotropy of single particle production relative to the reaction plane. Previous measurements [17] indicate that, even at large transverse momentum, the particle distributions contain an anisotropy due to elliptic flow that can be characterized by $dN/d(\phi-\Phi_r) \propto 1+2v_2\cos(2(\phi-\Phi_r))$, where Φ_r is the reaction plane angle determined event by event and v_2 is the elliptic flow parameter. This leads to a two particle azimuthal distribution of the form, $dN/d\Delta\phi = B(1+2v_2^2\cos(2\Delta\phi))$. The elliptic flow component of the two-particle azimuthal distribution is measured using several methods [17]. In this paper, v_2 is determined using a reaction-plane method.

A simple reference model can be constructed for the two-particle azimuthal distributions of high p_T particles in Au+Au collisions. A number of independent hard scatterings (each similar to one measured in a triggered p+p event) included in an event with correlations due to elliptic flow can be represented by the azimuthal distribution,

$$D^{\rm model} = D^{\rm pp} + B(1+2v_2^2\cos(2\Delta\phi)). \qquad (2)$$

The elliptic flow parameter (v_2) is measured independently in the same set of events, and is taken to be constant for $p_T > 2$ GeV/c [17]. The parameter B is then determined by fitting the observed $D^{\rm AuAu}$ in the region $0.75 < |\Delta\phi| < 2.24$ radians, which is largely free of jet contributions in the p+p data.

In Figure 2, the azimuthal distributions for $0 < |\Delta\eta| < 1.4$ in Au+Au collisions at various centralities are compared to Equation 2 using the measured p+p data. The centrality selection is constructed by subdividing the Au+Au minimum bias data sample into subsamples with different charged particle multiplicities within $|\eta| < 0.5$. The parameters v_2 and B are determined independently for each centrality bin, and are listed in Table I. For all centralities, the azimuthal correlation near $\Delta\phi = 0$ is well described by Equation 2. This indicates that the same mechanism (hard parton scattering and fragmentation) is responsible for high transverse momentum particle production in p+p and Au+Au collisions. However, the back-to-back correlations are suppressed in Au+Au collisions compared to the expectation from Equation 2, and the suppression is greater for more central collisions. The most central collisions show no indication of any back-to-back correlations beyond that expected from elliptic flow.

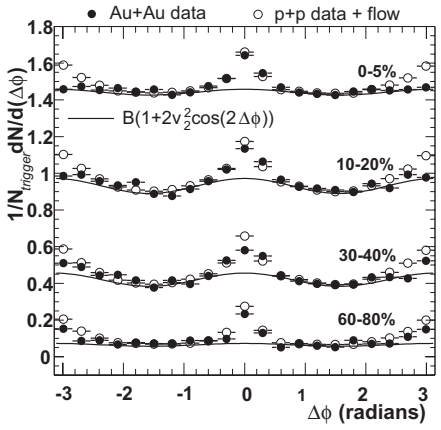

FIG. 2: Azimuthal distributions ($0 < |\Delta\eta| < 1.4$, $4 < p_T^{trig} < 6$ GeV/c) for Au+Au collisions (solid circles) compared to the expected distributions $D^{\rm model}$ from Equation 2 (open circles). Also shown is the elliptic flow contribution for each centrality (solid curve).

Centrality (%)	N_{part}	v_2	B
60-80	20±6	0.24±0.04	0.065± 0.003
40-60	61±10	0.22±0.01	0.231± 0.003
30-40	114±13	0.21±0.01	0.420± 0.005
20-30	165±13	0.19±0.01	0.633± 0.005
10-20	232±11	0.15±0.01	0.931± 0.006
5-10	298±10	0.10±0.01	1.187± 0.008
0-5	352±7	0.07±0.01	1.442± 0.003

TABLE I: Centrality, number of participants, v_2 ($2 < p_T < 6$ GeV/c), and normalization constant B. The errors on v_2 and B are statistical only, while the errors on the number of participants are systematic [14].

The ratio of the measured Au+Au correlation excess relative to the p+p correlation is:

$$I_{AA}(\Delta\phi_1,\Delta\phi_2) = \frac{\int_{\Delta\phi_1}^{\Delta\phi_2} d(\Delta\phi)[D^{\rm AuAu} - B(1+2v_2^2\cos(2\Delta\phi))]}{\int_{\Delta\phi_1}^{\Delta\phi_2} d(\Delta\phi) D^{\rm pp}}. \qquad (3)$$

The ratio can be plotted as a function of the number of participating nucleons (N_{part}), deduced from the centrality bins as described in reference [14]. I_{AA} is measured for both the small-angle ($|\Delta\phi| < 0.75$ radians) and back-to-back ($|\Delta\phi| > 2.24$ radians) regions. The ratio should

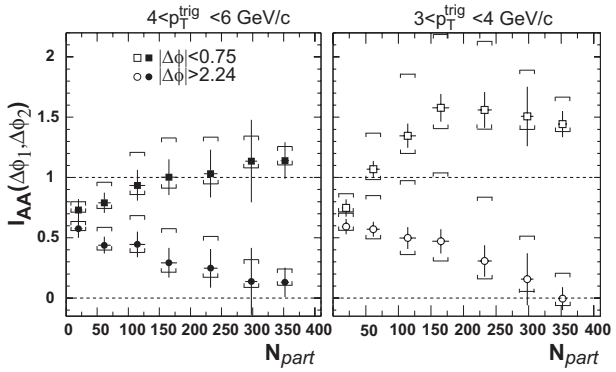

FIG. 3: Ratio of Au+Au and p+p (Equation 3) for small-angle (squares, $|\Delta\phi| < 0.75$ radians) and back-to-back (circles, $|\Delta\phi| > 2.24$ radians) azimuthal regions versus number of participating nucleons for trigger particle intervals $4 < p_T^{trig} < 6$ GeV/c (solid) and $3 < p_T^{trig} < 4$ GeV/c (hollow). The horizontal bars indicate the dominant systematic error (highly correlated among points) due to the uncertainty in v_2.

be unity if the hard-scattering component of Au+Au collisions is simply a superposition of p+p collisions unaffected by the nuclear medium. These ratios are given in Figure 3 for the trigger particle momentum ranges indicated. The asymmetric systematic errors are dominated by the +5/-20% systematic uncertainty on v_2 due to the potential non-flow contributions [20] as well as other sources of systematic uncertainty [17].

For the most peripheral bin (smallest N_{part}), both the small-angle and back-to-back correlation strengths are suppressed compared to the expectation from Equation 2. This may be an indication of initial state nuclear effects such as shadowing of parton distributions or scattering by multiple nucleons, or may be indicative of energy loss in a dilute medium [21]. As N_{part} increases, the small-angle correlation strength increases, with a more pronounced increase for the trigger particles with lower p_T threshold. If there were a large non-jet contribution to particle production (i.e. collective transverse flow) at the trigger threshold and above, it would dilute the jet related correlation signal and this ratio would be reduced. The back-to-back correlation strength, above background from elliptic flow, decreases with increasing N_{part} and is consistent with zero for the most central collisions. In the extreme case, if there were *no* elliptic flow for the 0-5% most central collisions, $I_{AA}(2.24, \pi) = 0.4 \pm 0.1$ for $4 < p_T^{trig} < 6$ GeV/c, compared to $I_{AA}(2.24, \pi) = 0.1 \pm 0.1$ using the measured elliptic flow value. Therefore, an overestimation of the elliptic flow cannot explain the observed suppression of back-to-back correlations.

Analyses of fixed-target experiments [22] have suggested that the shape of the back-to-back dihadron azimuthal distribution is sensitive to the intrinsic parton transverse momentum k_T in the initial state. In proton-nucleus and nucleus-nucleus collisions, additional initial-state transverse momentum can be generated by multiple nucleon-nucleon interactions preceding a hard scattering [23, 24, 25]. To investigate whether this nuclear k_T can account for the observed deficit of back-to-back azimuthal correlations in central Au+Au collisions, we have carried out Pythia [19] simulations varying the k_T parameter. A rather extreme change from the nominal value of $\sigma = 1$ GeV/c to 4 GeV/c introduced only a small effect, reducing the predicted $I_{AA}(2.24, \pi)$ by less than 20%. Experimental study of initial state effects on the azimuthal correlations requires the measurement of p(d)+Au collisions at RHIC energies.

In addition to the present data, two other striking effects have been observed at high p_T in nuclear collisions at RHIC: strong suppression of the inclusive hadron yield in central collisions [13, 14], and large elliptic flow which saturates at $p_T > 3$ GeV/c [17]. These phenomena are all consistent with a picture in which observed hadrons at $p_T > 3-4$ GeV/c are fragments of hard scattered partons, and partons or their fragments are strongly scattered or absorbed in the nuclear medium. The observed hadrons therefore result preferentially from hard-scattered partons generated on the periphery of the reaction zone and heading outwards [26]. In this picture the inclusive yield will be suppressed relative to the binary scaling expectation, and the strong position-momentum correlation required to explain the large elliptic flow [27] emerges naturally. The properties of small-angle hadron correlations will have weak dependence on the size of the colliding system, whereas the back-to-back correlations will exhibit strong suppression for a large system relative to a small one, both as observed.

In summary, STAR has measured azimuthal correlations for high p_T charged particles over a large relative pseudo-rapidity range with full azimuthal angle coverage. Comparison of the opposite-sign and same-sign correlation strengths indicates that hard scattering and fragmentation is the predominant source of charged hadrons with $p_T > 4$ GeV/c in central Au + Au collisions. The azimuthal correlations in Au+Au collisions have been treated as the superposition of independently determined elliptic flow and individual hard parton scattering contributions, the latter measured in the STAR p+p data. The most striking feature of the hard-scattering component is an increasing suppression of back-to-back relative to small-angle correlations with increasing centrality. These observations appear consistent with large energy loss in a system that is opaque to the propagation of high-momentum partons or their fragmentation products.

We wish to thank the RHIC Operations Group and the RHIC Computing Facility at Brookhaven National Laboratory, and the National Energy Research Scientific Computing Center at Lawrence Berkeley National Laboratory for their support. This work was supported by the Division of Nuclear Physics and the Division of High Energy Physics of the Office of Science of the U.S. Department of Energy, the United States National Science Founda-

tion, the Bundesministerium fuer Bildung und Forschung of Germany, the Institut National de la Physique Nucleaire et de la Physique des Particules of France, the United Kingdom Engineering and Physical Sciences Research Council, Fundacao de Amparo a Pesquisa do Estado de Sao Paulo, Brazil, the Russian Ministry of Science and Technology and the Ministry of Education of China and the National Natural Science Foundation of China.

[1] See for example: J.W. Harris and B. Müller, Annu. Rev. Nucl. Part. Sci. 46, 71 (1996).
[2] M. Gyulassy and M. Plümer, Phys. Lett. B243, 432 (1990).
[3] X. N. Wang and M. Gyulassy, Phys. Rev. Lett. 68, 1480 (1992).
[4] See for example: R. Baier, D. Schiff, and B. G. Zakharov, Annu. Rev. Nucl. Part. Sci. 50, 37 (2000).
[5] M. Banner *et al.*, Phys. Lett. B118, 203 (1982).
[6] G. Arnison *et al.*, Phys. Lett. B123, 115 (1983).
[7] F. Abe *et al.*, Phys. Rev. Lett. 62, 613 (1989).
[8] F. Abe *et al.*, Phys. Rev. D41, 1722 (1990).
[9] G. Arnison *et al.*, Phys. Lett. B118, 173 (1982).
[10] F. Abe *et al.*, Phys. Rev. Lett. 65, 968 (1990).
[11] T. Akesson *et al.*, Phys. Lett. B123, 133 (1983); J.A. Appel *et al.*, Phys. Lett. B160, 349 (1985); G. Arnison *et al.*, Phys. Lett. B172, 461 (1986); J.F. Owens, Rev. Mod. Phys. 59, 465 (1987).
[12] B. Brown *et al.*, Phys. Rev. Lett. 50, 11 (1983); R. Gomez *et al.*, Phys. Rev. D35, 2736 (1987); H. Miettinen *et al.*, Phys. Lett. B207, 222 (1988); R.C. Moore *et al.*, Phys. Lett. B244, 347 (1990).
[13] K. Adcox *et al.*, Phys. Rev. Lett. 88, 022301 (2002).
[14] C. Adler *et al.*, nucl-ex 0206011.
[15] C. Adler *et al.*, submitted to Nucl. Inst. Meth.
[16] G. Arnison *et al.*, Phys. Lett. B132, 223 (1983).
[17] C. Adler *et al.*, nucl-ex/0206006.
[18] P. Abreu *et al.*, Phys. Lett. B407, 174 (1997).
[19] T. Sjöstrand, P. Edén, C. Friberg, L. Lönnblad, G. Miu, S. Mrenna and E. Norrbin, Comp. Phys. Commun. 135, 238 (2001).
[20] C. Adler *et al.*, Phys. Rev. C66, 034904 (2002).
[21] F. Arleo, Phys. Lett. B532, 231 (2002); E. Wang and X.N. Wang, Phys. Rev. Lett. 89, 162301 (2002).
[22] L. Apanasevich *et al.*, Phys. Rev. Lett. 81, 2642 (1998).
[23] J.W. Cronin *et al.*, Phys. Rev. D11, 3105 (1975).
[24] M.D. Corcoran *et al.*, Phys. Lett. B259, 209 (1991).
[25] M. Lev and B. Petersson, Z. Phys. C21, 155 (1983).
[26] J.D. Bjorken, Fermilab-Pub-82/59-THY (1982).
[27] E.V. Shuryak, Phys. Rev. C66, 027902 (2002).